2

X-671-72-461
PREPRINT

OAO-2 OBSERVATIONS OF LY AUR

SARA R. HEAP

NOVEMBER 1972

GODDARD SPACE FLIGHT CENTER
GREENBELT, MARYLAND

X-671-72-461

OAO-2 OBSERVATIONS OF LY AUR

Sara R. Heap
Laboratory for Optical Astronomy

November 1972

Goddard Space Flight Center
Greenbelt, Maryland

ABSTRACT

The eclipsing binary, LY Aur (09.5 III) was observed over a period of four days in March 1972 with the Wisconsin instrumentation on OAO-2. Complete light curves were obtained at the following wavelengths: 4250, 3320, 2980, 2460, 1910, and 1550 Å. The phase resolution is usually 0.017.

A solution of each light curve was attempted according to the Russell-Merrill method, but no solution was found.

I. INTRODUCTION

Although LY Aur is a relatively bright object (V=6.7 to 7.3), it was not until 1968 that it was recognized by Mayer (1968) as an eclipsing binary as well as a double-lined spectroscopic binary. Because of its early spectral type (09.5 III), deep minima, and double-lined spectrum, LY Aur is potentially important for the determination of the masses and radii of hot, massive stars. Mayer and Horak (1972) give the following provisional parameters: $\mathcal{M}_1 = 24.7\mathcal{M}_\odot, R_1 = 10.5R_\odot$ and $\mathcal{M}_2 = 11.1\mathcal{M}_\odot, R_2 = 11.5R_\odot$.

In 1970, Commission 42 of the I.A.U. recommended a coordinated program of photometric measurements of LY Aur. So far, reports of UBV photometry have been given by Wood (1971), Mayer and Horak (1972), Hall and Heiser (1972), and Landolt and Blondeau (1972). The purpose of this paper is to report photoelectric photometry of LY Aur with the use of the Wisconsin Experiment (Code et al. 1970) on OAO-2. There are several features of this experiment which make it particularly useful for studying this binary system. First, it extends the wavelength range of measurements into the ultraviolet. Secondly it is capable of obtaining a complete light curve during the course of one period of the binary. This is especially helpful since the period of the binary, $4^d.002496$, is nearly an exact multiple of one earth day so that ground-based observations must be taken over

many cycles in order to obtain complete coverage of the light curve. Wood (1971), and Landolt and Blondeau (1972) have reported a slight variation in the light curve from cycle to cycle. Thirdly, it eliminates the problems due to the variability of the earth's atmospheric properties. In principle, the precision of the data is limited only by the precision of the detectors, which appears to better than one percent. In practice, however, the brightness of the sky surrounding LY Aur (i.e. the integrated brightness of all UV-emitting objects within the 10' field of view), although constant with time, is not known precisely, and this uncertainty generates small systematic distortions in the derived light curve.

Because the observations were made above the earth's atmosphere, the need for differential photometry is greatly lessened, and in fact, a comparison star was not used. The observations reported here consist of photometry of LY Aur and selected regions of the nearby sky. The following sections describe, in more detail, the methods of observation and reduction, and the results.

II. SCHEDULING OF OBSERVATIONS

Photoelectric photometry of LY Aur was obtained with the four 8-inch telescopes, which are part of the Wisconsin instrumentation on OAO-2. Each telescope has a field of view of 10 arc min. Of these telescopes, St 1, St 3, and St 4 were fully operative and were used to monitor the light variations of the binary at six wavelengths over the interval, 1550 Å to 4250 Å.

For clarity, the term, "observation," is used to denote the sequence of photometric measurements at a given orbit, and "measurement" is the number of counts registered at a specific wavelength by one of the photometers. Actually, a measurement consists of six determinations of the number of counts obtained after a specified integration time. A total of 42 observations of LY Aur and four observations of two nearby regions of the sky were scheduled during the nightime of nearly every orbit for four days in March 1972 (Orbits 17109 to 17161). The time resolution is therefore usually about 100 minutes, or equivalently, 0.017 in the phase of the binary. In 33 observations, the satellite was not over the South Atlantic portion of the earth, and observations could be scheduled for the full duration of nightime. In these cases, two measurements each were obtained at λ4250, λ3320, λ2980, and one measurement was obtained at λ2460, λ1980, λ1550 and of the calibration source. In the remaining observations, the scheduled observing sequence had to be shortened because of the South Atlantic Anomaly, and one measurement was obtained only at

λ4250, λ3320, λ2460, λ1550.

The sky near LY Aur was sampled again in April 1972 because of ambiguity in the sky data obtained in March. The two Sky's observed earlier (Sky 1 and Sky 2) were re-observed, and two additional regions of the sky near LY Aur were observed (Sky 3 and Sky 4). The 1950 coordinates of LY Aur and the four Sky's are listed in Table 1.

III. REDUCTIONS

The universal time of each measurement was derived from the formula,

$$t = t_o + 6^s + \Delta t/2, \qquad (1)$$

where t_o is the U.T. time at the scheduled start of each measurement, 6 sec is the time alloted to set the filters, and Δt is the total integration time. The U.T. time of each measurement should be accurate to $\pm$ 3 sec. The U.T. time was converted to heliocentric Julian date, and the phase was computed with the use of Mayer and Horak's (1972) elements:

$$\text{PRI. MIN.} = \text{J.D. hel. } 243\,9061.463 + 4^d.002496. \qquad (2)$$

Let 1' be the count rate of the star corrected for the effects of dark current, sky background, and variations in the sensitivity of the equipment from orbit to orbit. It is given by,

$$1' = \left[(\text{STAR-DARK}) - (\overline{\text{SKY-DARK}})\right] \times \frac{(\overline{\text{CAL-DARK}})}{(\overline{\text{CAL-DARK}})} \qquad (3)$$

Here, (STAR-DARK), (SKY-DARK), and (CAL-DARK) are the counts per second above dark registered by the star at a given measurement, the adopted sky background, and the estimated calibration source at that orbit, respectively. (Hereafter, 1' refers to the luminosity of the system in counts per sec, while 1 refers to the luminosity of the system normalized to one at maximum.)

The observing sequence scheduled for each orbit was set up so that measurements of the dark current were taken

on all photometers at the beginning and end of each observation. In addition, a third measurement of the dark current was taken in the middle of the observing sequence on St 1. The variation of the dark current during the course of an observation was negligible on St 3 and St 4, so the mean of the two measured DARK'S was used to represent DARK at each measurement. On St 1, the intensity of the dark current dropped steadily between the beginning and end of the observing sequence. The value of DARK at the time of a STAR or CAL measurement was estimated under the assumption that the dark current varied linearly with time. Comparison of the computed DARK with the measured DARK taken in the middle of the observation confirms this assumption.

The adopted value of (SKY-DARK) was the mean brightness of Sky 2, Sky 3, and Sky 4. Sky 1 was not used in the average because it appeared anomalously bright compared to the other three Sky's, including Sky 4 whose field of view partially overlaps that of Sky 1. Table 2 gives the adopted value of $\overline{\text{SKY-DARK}}$ and the standard deviation of the mean.

Measurements of the calibration source were taken on 33 orbits. These measurements indicate a small systematic trend of sensitivity with time, as shown in Figure 1. The smooth curve in this figure represents a third-degree polynomial which was fitted to the data in a least-squares sense.

Since an observed value of (CAL-DARK) was not available at every orbit, the least-squares (CAL-DARK) was used in Eq. 3. Table 3 gives information relevant to the calibration. Successive columns list the photometer, mean value of (CAL-DARK) and the standard deviation of a single measurement, the standard deviation of a single measurement for the computed (CAL-DARK), and the average standard deviation of CAL as determined from the six individual determinations that constitute a given measurement.

The count rates were converted to magnitudes according to,

$$m = -2.5 \log 1' + \Delta m_f - C. \qquad (4)$$

Here, C is a normalizing constant such that the average value of m during the phase intervals, 0.23 - 0.27P and 0.73 - 0.77P, is zero. The value of C at each filter is given in Table 4. The term, Δm_f, accounts for the degradation of the filter during the four days of observation. It is zero except at λ1550.

The λ1550 filter has been degrading steadily since Orbit 8000, but it appears to have plummited sometime between Orbit 17100 and Orbit 17300 and then to have leveled off somewhat after Orbit 17300. Leckrone's (1972) degradation study indicates the <u>average</u> rate of degradation was 0.0165 mag per day between Orbit 17100 and 17300. However, when this value was used, the light curve at λ1550 showed

serious asymmetries. An alternate rate of degradation was estimated by forcing all counts at maximum light to be equal. This derived rate of 0.0279 mag per day was used in equation (4) for λ1550 data. As will be seen in §V, this value produces symmetrical eclipse branches, like those at the other filters, so there is reason to be confident in this correction factor.

IV. OBSERVATIONAL RESULTS

Tables 5 (a) - 5 (f) give the heliocentric Julian date, the normalized magnitude, and phase of each filter. On 33 orbits two measurement of STAR were taken on St 1. These second measurements are listed separately after the first measurement.

Since the observing technique differs considerably from that of ground-based photometry, it is worthwhile to consider the uncertainties in the data. There are four main sources of error: noise in the data, errors in estimating the dark current, variations in the sensitivity of the equipment, and uncertainty in the brightness of the sky immediately around LY Aur. Below, each source of error is considered separately, and the magnitude of its effect on 1' is estimated.

As noted earlier, each measurement of STAR, SKY, DARK, or CAL is actually the mean of six individual determinations. The standard error of the mean of the six determinations, σ (STAR), was calculated for all measurements of STAR and the average is listed in column 3 of Table 6. For comparison, the value of 1' at maximum light, $1'_{max} = 10^{-0.4\ C}$, is given in column 2. Several measurements of STAR had large errors, σ (STAR) > 2 $<\sigma$ (STAR)>. These are noted in Table 5 by a semi-colon.

The uncertainty in the calibration, as given by the ratio, σ_{sm} (CAL-DARK)$_c$ / (CAL-DARK), places the following

limitations on the precision of the measurements: 0.5% on St 1 (λ4250, λ3320, λ2980), 0.4% on St 3 (λ2460, λ1910), and 0.5% on St 4 (λ1550). The resulting uncertainty in 1' was evaluated at maximum light. It is listed in column 4 of Table 6.

Since σ_{sm} (CAL-DARK), is approximately the same as $\langle\sigma$ (CAL)$\rangle$, it is reasonable to assume that the errors in estimating the dark current are negligible.

As described earlier, the adopted value of (SKY-DARK) is the average of measurements of Sky 2, Sky 3, and Sky 4. The standard error of the mean, σ ($\overline{\text{SKY-DARK}}$), is given in column 5 of Table 6. Unlike the other errors, the uncertainty in the sky produces a systematic error, distorting the light curve in the same way as would light from a third component.

In summary, the photometry of LY Aur is better than 1% at all filters, when accidental errors are considered. The uncertainty of the sky background adds an additional systematic error, especially at λ4250 where the uncertainty of the sky brightness is particularly large relative to the brightness of the system. In addition, the light curve at λ1550 is less reliable than the rest because of the problem of degradation of that filter.

V. LIGHT CURVES

Light curves at each filter ($l = 10^{-0.4m}$ vs. phase) are shown in Figures 2 and 3. Since there are no indications of asymmetry, phases from 0.5 to 1.0 are reversed in these figures. The results at phases from 0.0 to 0.5 are indicated by a dot, while phases from 0.5 to 1.0 are noted by a cross.

The light outside eclipse was expressed by the truncated Fourier series:

$$l_{out}(\theta) = \sum_{n=o}^{4} A_n \cos n\theta + \sum_{n=1}^{2} B_n \sin n\theta, \qquad (5)$$

It was assumed that the angle of external tangency, $\theta_e = 45^o$, but any value of θ_e from about 37^o to 45^o yields the same coefficients since the angular resolution of the data is nearly 8^o. Each measurement was given unit weight. Table 7 gives the least-squares values of the coefficients. It is important to note that at most filters, the coefficients of the sine terms and the higher-order cosine terms are smaller than the observational uncertainty due to calibration and noise combined (cf. Table 6).

The coefficients at λ4250 were recomputed using only the cosine terms and were compared with those computed by Mayer and Horak from their observations at the B filter. They obtain a greater distortion of the system ($A_1 = +0.0091$, $A_2 = -0.1334$), while the OAO observations yield $A_1 = +0.0079$ $A_2 = -0.1220$. This discrepancy cannot be explained by a

possibly poor value of the sky brightness obtained with the OAO: changing the sky brightness from the adopted 148 counts per sec by ± 8 counts per sec (cf. Table 2) yields a change in the coefficients, $\Delta A_1 = \pm 0.0001$ $\Delta A_2 = \pm 0.006$. A more likely cause of the difference is that Mayer and Horak's observations of maximum are incomplete, having gaps between 0.19 and 0.40P and between 0.64 and 0.74P.

Mayer and Horak report that primary minimum is an occultation lasting about 100 minutes, or equivalently, ± 0.0087 in phase. It was therefore assumed that the two OAO observations at approximately ± 0.009P were made just at the edge of totality, so that they serve to define primary minimum. The light curve during secondary eclipse was extrapolated by eye to obtain the light at secondary minimum. Table 8 lists the observed depths at primary and secondary minimum, respectively.

The coefficients of Table 7 were used to rectify the light curve at each filter according to standard procedures (Binnendijk 1970), and an attempt was made to solve for the photometric elements of the system. However, no solution would be found at any filter, i.e. depths and shapes of the eclipses yield inconsistent solutions.

VI. ATMOSPHERIC PROPERTIES OF THE LARGER STAR

A IIaO spectrogram of LY Aur at 13.3Å/mm was obtained in March 1972 at the 84-inch telescope at Kitt Peak Observatory. The central time of the observation was J.D. hel = 2441406.68, and the phase was 0.94. According to the λ4250 light curve, radiation from the larger star contributes about three-fourths of the observed intensity, so it was assumed that the spectrum is essentially that from the larger star.

Equivalent widths of several hydrogen and helium lines were measured and are listed in Table 9. Comparison of the measured ratios of equivalent width, HI/HeI and HeII/HeI, with those computed by Auer and Mihalas (1972) from their non-LTE models yield $T_e = 30{,}000^{\circ}$ and log g = 3.5 for the larger star. This is entirely consistent with the 09.5 III spectral type of LY Aur.

VII. INTERSTELLAR EXTINCTION

The observed flux distribution and atmospheric parameters of the larger star were used to estimate the wavelength dependence of interstellar extinction, $X_\lambda = E(\lambda - V)/E(B - V)$. The value of X_λ was computed according to

$$X_\lambda = \frac{(m_\lambda - m_B) - (m_\lambda - m_B)_o}{E(B-V)} + 1. \qquad (6)$$

The term $(m_\lambda - m_B)$ was obtained from the magnitudes of the six filters during primary minimum and calibration constants for each filter derived by Code (1970) and Leckrone (1972) for orbit 17100. The term $(m_\lambda - m_B)_o$ was computed from Mihalas' (1972) tables of fluxes. The average flux of the $T_e = 30{,}000^o$, log g = 4.0 model and the $T_e = 30{,}000^o$, log g = 3.0 model was used to represent flux distribution of the larger component of LY Aur. Mayer and Horak's (1972) observations indicate that at primary minimum, B-V = + 0.21, which implies that E (B-V) $\approx$ 0.44. Successive columns of Table 10 give the wavelength of each filter, the observed $(m_\lambda - m_B)$ of the larger star, the intrinsic $(m_\lambda - m_B)_o$, and the derived value of X_λ. Although the extinction curve for LY Aur falls within the envelope of curves which Bless and Savage (1972) found, it deviates considerably from their average extinction curve, being up to $0^m.5$ smaller at λ2980 and 2460 and $0^m.5$ larger at λ1550 than the average. This difference cannot be ascribed to any one cause, but is probably the result of several factors, e.g.

the use of a non-blanketed non-LTE model to represent the star, observational error, uncertainty in the intrinsic $(B-V)_o$ of LY Aur and consequently, in E(B-V), and variations in X_λ in different regions of the galaxy.

ACKNOWLEDGEMENTS

I would like to thank Drs. D. S. Leckrone, W. M. Sparks, and D. K. West for their help in scheduling the OAO observations, and the NASA and Grumman personnel for operating the spacecraft in difficult circumstances. I appreciated helpful conversations with Drs. A. V. Holm and S. Sobieski concerning the reduction of the data. I also wish to thank Dr. A. Hoag and Mr. S. Levy of Kitt Peak National Observatory for their assistance in obtaining the visual spectra.

REFERENCES

Auer, L. H., and Mihalas, D. M. 1972, Ap. J. Suppl. No. 205.

Binnendijk, L. 1970, in Vistas in Astronomy, ed. A. Beer (New York: Pergamon Press), p. 217.

Bless, R. C., and Savage, B. D. 1972, Ap. J. 171, 293.

Code, A. D. 1970, Priv. communication.

Code, A. D., Houck, T. E., McNall, J. F., Bless, R. C., and Lillie, C. F. 1970, Ap. J. 161, 377.

Hall, D. S., and Heiser, A. M. 1972, P.A.S.P. 84, 33.

Landolt, A.U., and Blondeau, K. L. 1972, P.A.S.P. 84, 394.

Leckrone, D. S. 1972, priv. communication.

Mayer, P. 1968, P.A.S.P. 80, 81.

Mayer, P., and Horak, T. B. 1972, B.A.C. 22, 327.

Mihalas, D. M. 1972, NCAR Tech. Note STR-76, National Center for Atmospheric Research, Boulder, Colorado.

FIGURE CAPTIONS

Fig. 1 - Measured (CAL-DARK) on the three photometers, St 1, St 2, and St 3.

Fig. 2 - Light curve of LY Aur at λ4250, λ3320, and λ2980. The ordinate gives the light in intensity units, normalized to one at maximum. The abscissa gives the phase. Phases from 0.5 to 1.0 are reversed. The results at phases from 0.0 to 0.5 are shown by a dot, while those at phases from 0.5 to 1.0 are noted by a cross.

Fig. 3 - Light curve of LY Aur at λ2460, λ1910, and λ1550.

TABLE 1

1950 COORDINATES OF STAR AND SKY'S

Object	α	δ
LY Aur	$05^h\ 26^m.38$	$+35^\circ\ 20'.2$
Sky 1	05 26.38	+35 35.2
Sky 2	05 26.58	+35 10.0
Sky 3	05 27.38	+35 20.3
Sky 4	05 25.88	+35 30.3

TABLE 2

OBSERVED BRIGHTNESS OF THE SKY

λ (Å)	SKY-DARK (counts per sec)	σ (counts per sec)
4250	148.	± 8.3
3320	13.7	0.23
2980	10.2	0.81
2460	2.71	0.50
1910	0.289	0.077
1550	0.139	0.006

TABLE 3

CALIBRATION DATA

PHOTOMETER	$\overline{\text{CAL-DARK}}$ [cps]	σ_{sm} $(\overline{\text{CAL-DARK}})$ [cps]	σ_{sm} $(\text{CAL-DARK})_c$ [cps]	$\langle\sigma\,(\text{CAL})\rangle$ [cps]
ST1	139.5	$\pm$0.8	$\pm$0.7	$\pm$0.6
ST3	231.6	1.1	0.8	0.9
ST4	128.5	0.9	0.7	0.7

TABLE 4

NORMALIZING CONSTANTS

λ (Å)	C (mag)
4250	-7.024
3320	-5.788
2980	-5.660
2460	-4.348
1910	-2.441
1550	-0.206

TABLE 5(a)

OBSERVATIONS AT 4250Å

J.D. hel. [2441300+]	m [mag]	Phase	J.D. hel. [2441300+]	m [mag]	Phase
87.6118	0.036	0.175	87.8913	$^{-}$0.004	0.244
87.6814	0.019	0.192	87.9616	$^{-}$0.009	0.262
87.7515	$_{-}$0.011	0.209	88.0309	0.001	0.279
87.8846	$^{-}$0.005	0.243	88.1004	0.013	0.297
87.9549	$^{-}$0.006	0.260	88.1698	0.015	0.314
88.0242	0.004	0.278	88.3094	0.054	0.349
88.0937	0.011	0.295	88.3788	0.074	0.366
88.1631	0.011	0.312	88.5177	0.151	0.401
88.3027	0.061	0.347	88.8662	0.540	0.488
88.3720	0.079	0.364	88.9358	0.554	0.505
88.5110	0.134	0.399	89.0051	0.509	0.523
88.6554	0.285	0.435	89.0746	0.430	0.540
88.7250	0.385	0.453	89.2135	0.244	0.575
88.8595	0.536	0.486	89.2830	0.175	0.592
88.9290	0.545	0.504	89.4224	0.100	0.627
88.9984	0.517	0.521	89.8399	$_{-}$0.009	0.731
89.0679	0.431	0.538	89.9092	$^{-}$0.001	0.749
89.2067	0.254	0.573	89.9795	0.006	0.766
89.2763	0.181	0.590	90.0487	0.012	0.783
89.4157	0.104	0.625	90.1876	0.020	0.818
89.6291	0.037	0.679	90.2571	0.042	0.835
89.6984	$_{-}$0.021	0.696	90.3966	0.092	0.870
89.8331	$^{-}$0.014	0.730	90.8133	0.590	0.974
89.9025	0.013:	0.747	90.8837	0.689	0.992
89.9727	0.012	0.764	90.9530	0.671	0.009
90.0420	0.019	0.782	91.0223	0.565	0.027
90.1809	0.030	0.816	91.0917	0.441	0.044
90.2504	0.028	0.834	91.1610	0.327	0.061
90.3899	0.088	0.869	91.3006	0.157	0.096
90.6726	0.348	0.939			
90.7429	0.458	0.957			
90.8066	0.645	0.973			
90.8769	0.692	0.990			
90.9463	0.667	0.008			
91.0156	0.575	0.025			
91.0850	0.476	0.042			
91.1543	0.400:	0.060			
91.2939	0.158	0.095			

NOTE: Table 5 was generated via an APL/360 program stored on an IBM 360/95. This program prints a negative sign as a superscript.

TABLE 5(b)

OBSERVATIONS AT 3320Å

J.D. hel. [2441300+]	m [mag]	Phase	J.D. hel. [2441300+]	m [mag]	Phase
87.6069	0.034	0.173	87.8924	−0.002	0.245
87.6765	0.016	0.191	87.9627	−0.001	0.262
87.7466	0.002	0.208	88.0320	−0.012	0.280
87.8860	−0.009	0.243	88.1015	0.010	0.297
87.9563	−0.007	0.261	88.1709	0.020	0.314
88.0257	−0.013	0.278	88.3105	0.062	0.349
88.0952	0.003	0.295	88.3799	0.075	0.366
88.1645	0.025	0.313	88.5188	0.165	0.401
88.3041	0.058	0.348	88.8673	0.555	0.488
88.3735	0.087	0.365	88.9369	0.556	0.506
88.5125	0.154	0.400	89.0062	0.515	0.523
88.5805	0.214	0.417	89.0757	0.431	0.540
88.6505	0.284	0.434	89.2146	0.261	0.575
88.7201	0.359	0.451	89.2841	0.186	0.592
88.8609	0.544	0.487	89.4235	0.107	0.627
88.9305	0.554	0.504	89.8410	0.006	0.731
88.9998	0.516	0.521	89.9103	0.009	0.749
89.0694	0.433	0.539	89.9806	0.004	0.766
89.2082	0.268	0.573	90.0498	0.005	0.784
89.2777	0.182	0.591	90.1887	0.044	0.818
89.4172	0.108	0.626	90.2582	0.049	0.836
89.5539	0.071	0.660	90.3977	0.098	0.871
89.6242	0.040	0.677	90.8144	0.623	0.975
89.6935	0.025	0.695	90.8848	0.699	0.992
89.8346	0.010	0.730	90.9541	0.692	0.010
89.9039	0.002	0.747	91.0234	0.586	0.027
89.9742	0.005	0.765	91.0928	0.458	0.044
90.0435	0.006	0.782	91.1621	0.351	0.062
90.1824	0.037	0.817	91.3017	0.158	0.096
90.2519	0.052	0.834			
90.3913	0.099	0.869			
90.5268	0.190	0.903			
90.5983	0.249:	0.921			
90.6677	0.348	0.938			
90.7379	0.465	0.956			
90.8080	0.600	0.973			
90.8784	0.696	0.991			
90.9477	0.681	0.008			
91.0171	0.589	0.025			
91.0864	0.455	0.043			
91.1558	0.344	0.060			
91.2954	0.154	0.095			

TABLE 5(c)

OBSERVATIONS AT 2980Å

J.D. hel. [2441300+]	m [mag]	Phase	J.D. hel. [2441300+]	m [mag]	Phase
87.8850	0.012	0.243	87.8917	0.001	0.244
87.9552	0.003	0.260	87.9620	0.003	0.262
88.0246	0.016	0.278	88.0313	0.015	0.279
88.0941	0.003	0.295	88.1008	0.007	0.297
88.1634	0.009:	0.312	88.1702	0.004	0.314
88.3030	0.039	0.347	88.3098	0.043	0.349
88.3724	0.070	0.365	88.3791	0.076	0.366
88.5114	0.152	0.399	88.5181	0.157	0.401
88.8598	0.551	0.486	88.8666	0.564	0.488
88.9294	0.553	0.504	88.9361	0.554	0.505
88.9987	0.511	0.521	89.0055	0.510	0.523
89.0683	0.428	0.538	89.0750	0.424	0.540
89.2071	0.266	0.573	89.2138	0.244	0.575
89.2766	0.183	0.590	89.2834	0.180	0.592
89.4161	0.119	0.625	89.4228	0.098	0.627
89.8335	0.015	0.730	89.8402	0.005	0.731
89.9029	0.013	0.747	89.9096	0.004	0.749
89.9731	0.004	0.765	89.9798	0.009	0.766
90.0424	0.017	0.782	90.0491	0.021	0.783
90.1813	0.046	0.817	90.1880	0.041	0.818
90.2508	0.050	0.834	90.2575	0.053	0.836
90.3902	0.097	0.869	90.3970	0.096	0.870
90.8069	0.604	0.973	90.8137	0.609	0.975
90.8773	0.725	0.990	90.8840	0.740	0.992
90.9466	0.720	0.008	90.9534	0.709	0.009
91.0160	0.615	0.025	91.0227	0.600	0.027
91.0853	0.490	0.042	91.0921	0.474	0.044
91.1547	0.370	0.060	91.1614	0.361	0.061
91.2943	0.174	0.095	91.3010	0.158	0.096

TABLE 5(d)

OBSERVATIONS AT 2460Å

J.D. hel. [2441300+]	m [mag]	Phase
87.6094	0.046	0.174
87.6790	0.025	0.191
87.7491	0.016	0.209
87.8890	0.006	0.244
87.9592	-0.003	0.261
88.0286	-0.003	0.279
88.0981	0.007	0.296
88.1674	0.018	0.313
88.3070	0.057	0.348
88.3764	0.079	0.366
88.5154	0.161	0.400
88.5831	0.225	0.417
88.6531	0.304:	0.435
88.7226	0.397	0.452
88.8638	0.572	0.487
88.9334	0.581	0.505
89.0027	0.544	0.522
89.0723	0.455:	0.539
89.2111	0.269	0.574
89.2806	0.196	0.591
89.4201	0.112	0.626
89.5565	0.080	0.660
89.6267	0.056	0.678
89.6961	0.025	0.695
89.8375	-0.032	0.731
89.9069	-0.009	0.748
89.9771	-0.001	0.766
90.0464	-0.002	0.783
90.1853	0.036	0.818
90.2548	0.049	0.835
90.3943	0.109	0.870
90.5294	0.203	0.903
90.6009	0.280	0.921
90.6702	0.383	0.939
90.7405	0.503	0.956
90.8109	0.646	0.974
90.8813	0.764	0.991
90.9507	0.767	0.009
91.0200	0.633	0.026
91.0893	0.494	0.043
91.1587	0.374	0.061
91.2983	0.180	0.096

TABLE 5(e)

OBSERVATIONS AT 1910Å

J.D. hel. [2441300+]	m [mag]	Phase
87.8852	-0.009	0.243
87.9555	0.005	0.260
88.0248	-0.006	0.278
88.0943	0.014	0.295
88.1637	0.027	0.312
88.3033	0.063	0.347
88.3726	0.087	0.365
88.5116	0.169	0.399
88.8601	0.577	0.486
88.9296	0.557	0.504
88.9990	0.538	0.521
89.0685	0.441	0.538
89.2073	0.249	0.573
89.2769	0.223	0.591
89.4163	0.096:	0.625
89.8337	0.018	0.730
89.9031	0.007	0.747
89.9733	-0.004	0.765
90.0426	0.034	0.782
90.1815	0.057	0.817
90.2510	0.077	0.834
90.3905	0.132	0.869
90.8072	0.676	0.973
90.8775	0.819	0.990
90.9469	0.798	0.008
91.0162	0.696	0.025
91.0856	0.550	0.042
91.1549	0.424	0.060
91.2945	0.224	0.095

TABLE 5(f)

OBSERVATIONS at 1550Å

J.D. hel. [2441300+]	m [mag]	Phase
87.6094	0.057	0.174
87.6790	-0.012	0.191
87.7491	-0.002	0.209
87.8890	-0.005	0.244
87.9592	-0.000	0.261
88.0286	-0.002	0.279
88.0981	0.017	0.296
88.1674	0.027	0.313
88.3070	0.058	0.348
88.3764	0.081	0.366
88.5154	0.201	0.400
88.5831	0.236	0.417
88.6531	0.311	0.435
88.7226	0.360	0.452
88.8638	0.525	0.487
88.9334	0.533	0.505
89.0027	0.492	0.522
89.0723	0.435	0.539
89.2111	0.257	0.574
89.2806	0.198	0.591
89.4201	0.134	0.626
89.5565	0.092	0.660
89.6267	0.068	0.678
89.6961	-0.025	0.695
89.8375	-0.001	0.731
89.9069	0.006	0.748
89.9771	0.016	0.766
90.0464	0.035	0.783
90.1853	0.053	0.818
90.2548	0.084	0.835
90.3943	0.138	0.870
90.5294	0.220	0.903
90.6009	0.286	0.921
90.6702	0.411	0.939
90.7405	0.508	0.956
90.8109	0.656	0.974
90.8813	0.749	0.991
90.9507	0.729	0.009
91.0200	0.647	0.026
91.0893	0.498	0.043
91.1587	0.392	0.061

TABLE 6

EVALUATION OF VARIOUS ERRORS

λ (Å)	$1'_{max}$ (cps)	$\langle\sigma(\text{STAR})\rangle$ (cps)	$1'_{max}$ $\sigma_{(CAL-DARK)c}$ $\overline{(CAL-DARK)}$ (cps)	$\sigma(\overline{SKY-DARK})$ (cps)
4250	645	$\pm$1.9	$\pm$3.2	$\pm$8.3
3320	207	0.8	1.0	0.2
2980	184	0.7	0.9	0.8
2460	54.8	0.04	0.2	0.5
1910	9.49	0.06	0.03	0.08
1550	1.21	0.007	0.006	0.006

TABLE 7

FOURIER COEFFICIENTS OF LIGHT AT MAXIMUM

λ (Å)	A_o	A_1	A_2	A_3	A_4	B_1	B_2
4250	+0.8995	+0.0044	-0.1137	+0.0024	-0.0139	+0.0027	-0.0024
3320	+0.9080	-0.0015	-0.0963	-0.0012	-0.0017	+0.0059	-0.0017
2980	+0.8973	+0.0137	-0.1146	+0.0155	-0.0125	+0.0056	-0.0051
2460	+0.8903	-0.0306	-0.1166	-0.0151	-0.0077	+0.0029	-0.0098
1910	+0.9080	-0.0257	-0.0834	-0.0058	+0.0073	+0.0067	+0.0041
1150	+0.8914	-0.0252	-0.1050	-0.0090	+0.0037	+0.0106	-0.0026

TABLE 8

DEPTHS OF MINIMA

λ [A]	D (PRI. MIN.)	D (SEC. MIN.)
4250	0.42	0.41
3320	.45	.41
2980	.48	.41
2460	.51	.43
1910	.53	.42
1550	.50	.40

TABLE 9

MEASURED EQUIVALENT WIDTHS

Ion	λ [Å]	W_λ [Å]
HY	4340	2.10
HeI + HeII	4026	0.94
HeI	4387	0.50
HeI	4471	0.78
HeII	4542	0.38

TABLE 10

INTERSTELLAR EXTINCTION

λ	$(m_\lambda - m_B)$	$(m_\lambda - m_B)$	X_λ
4250	$0^m.00$	$0^m.00$	1.0
3320	-0.42	-0.76	1.8
2980	-0.53	-1.14	2.4
2460	-0.58	-1.79	3.8
1910	-0.82	-2.63	5.1
1550	-1.48	-3.23	4.9

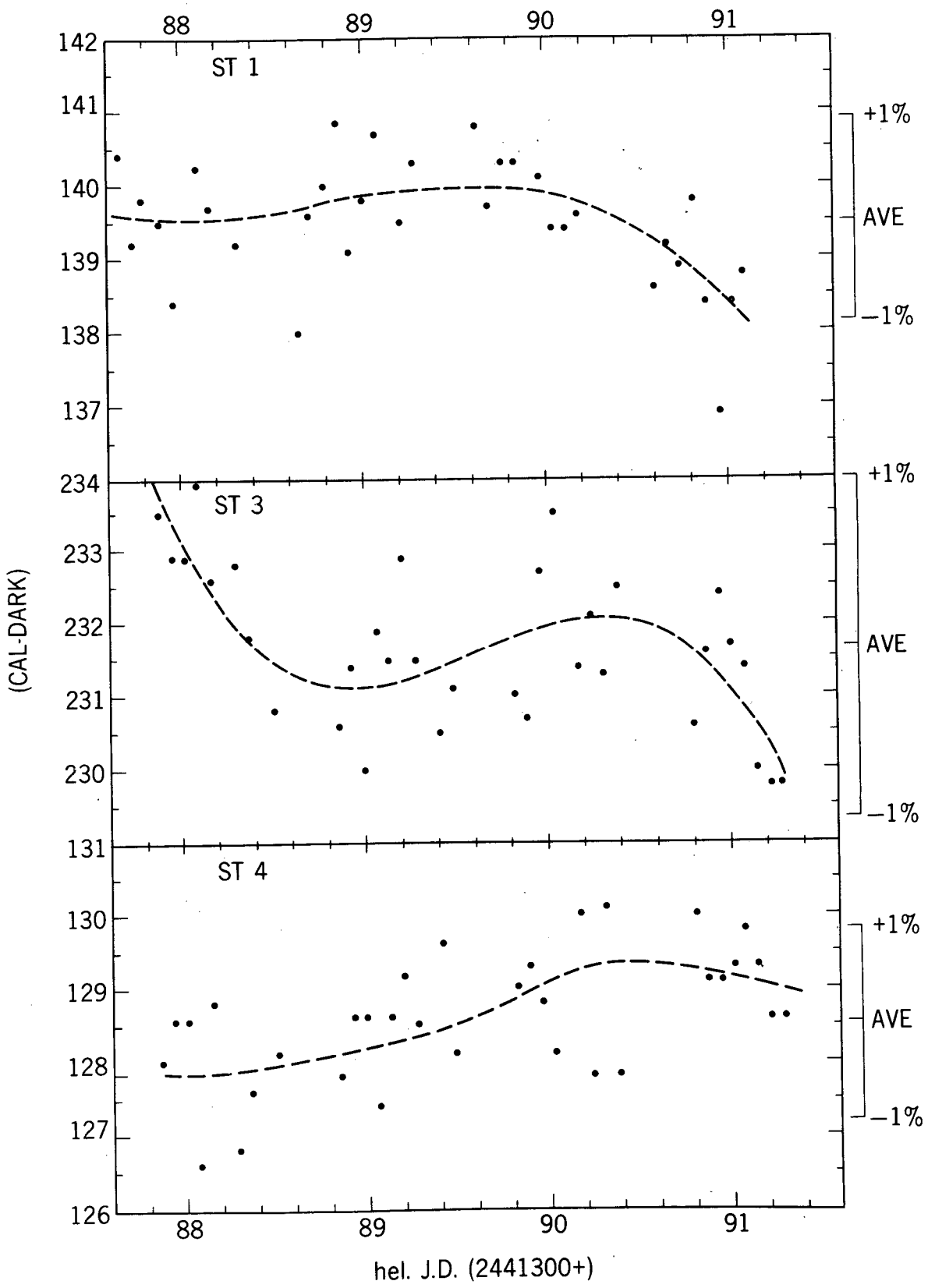
88
89
90
91
142
141
140
139
138
137
ST 1
+1%
AVE
−1%
234
233
232
231
230
ST 3
+1%
AVE
−1%
131
130
129
128
127
126
ST 4
+1%
AVE
−1%
(CAL-DARK)
hel. J.D. (2441300+)

FIG. 1

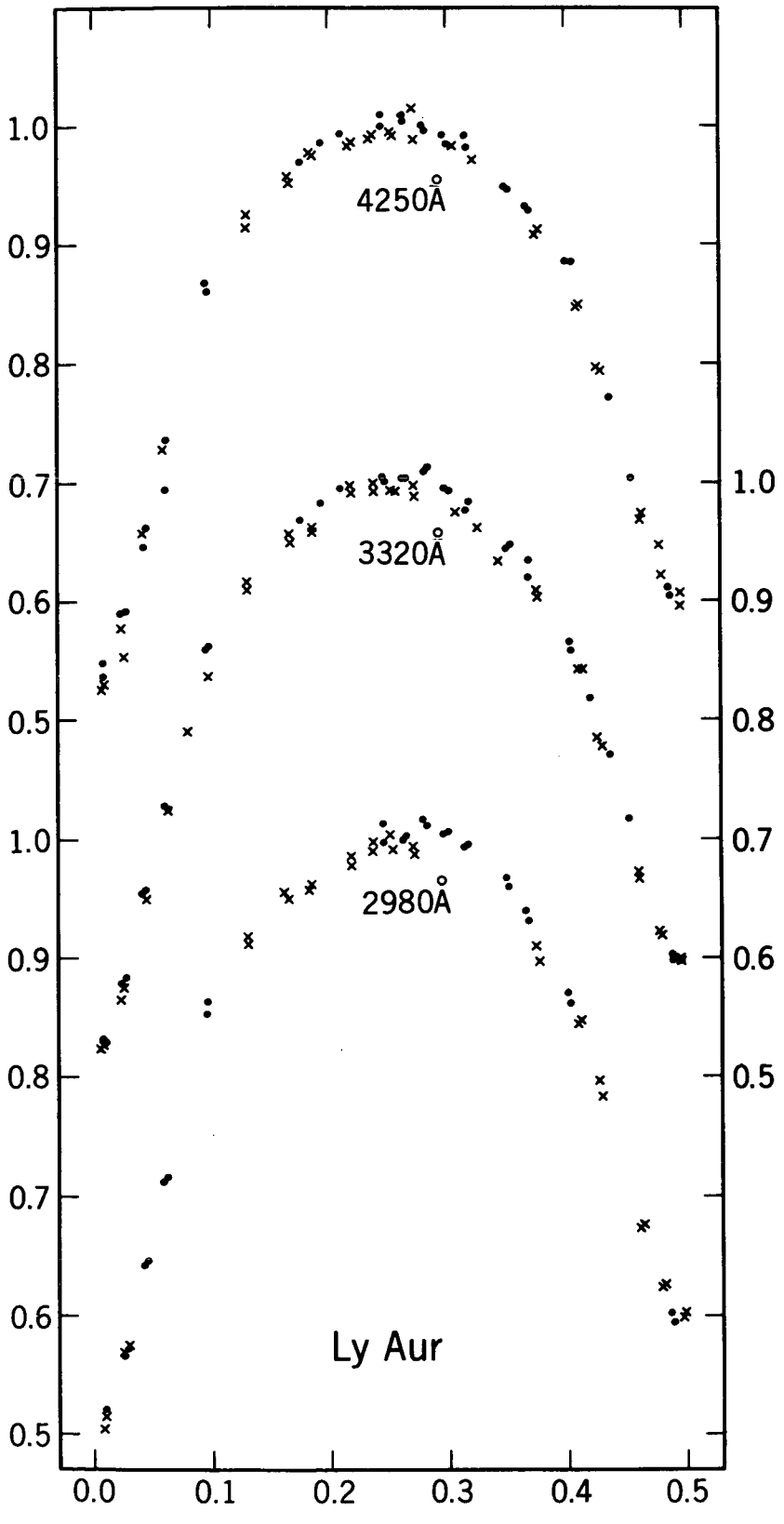

FIG. 2

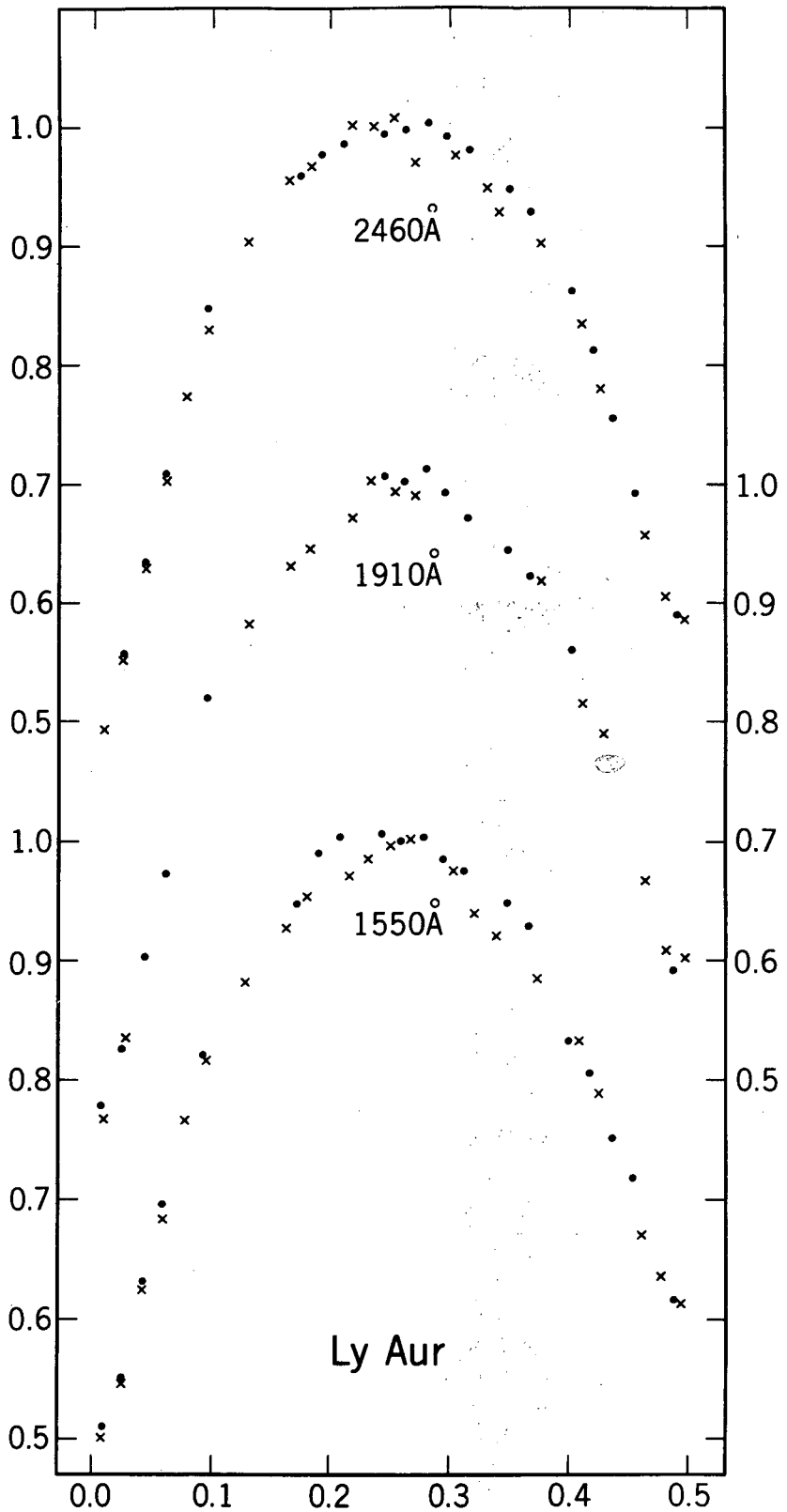

NASA–GSFC

FIG. 3